International Journal of Recent Technology and Engineering (IJRTE)
ISSN: 2277-3878, Volume-8 Issue-3, September 2019

Synthesis of alloying Al 7075 with Molybdenum for Functional Characterization

A. Haja Maideen, Muthukannan Duraiselvam, M. Varatharajulu

Abstract: ***Alloying was conducted on Al 7075 alloy by reinforcement of the metallic portion of molybdenum (Mo) in po wder blended with dielectric fluid to strengthen wear resistance a nd investigate the lubing features of this woven surface. The present work features alloying of Al 7075 with Mo as a vital material. Mechanical attributes along with powder frustration and layered coating size and shape were investigated by scanning electron microscope (SEM), energy dispersive X-ray analysis (EDXA), optical microscope (OM), surface texture with roughness tester and wear vision using pin on disc device. The effect of Peak current (A), Pulse on time (P_{on}) and Pulse off time (P_{off}) on the wear execution of an alloyed discharge, Al 7075 auxiliary materials have also been considered using Response Surface Methodology (RSM). Analysis of Variance (ANOVA) was interpreted to add to the effectiveness of material variables on the performance characteristics. Confirmation tests were performed to compare the predicted values with the experimental values and it was found that the results matched well with the experimental results.***

Keywords: Electrical discharge alloying, Surface roughness, Specific wear rate, Coefficient of friction, RSM Technique.

I. INTRODUCTION

Because of its most amazing quality, aluminum (Al) 7000 series alloys are being used as supporting structure for many design applications such as aviation, sports equipment as well as in automotive industries. These Al amalgam arrangement substitute heavier designing materials because of its better quality than thickness proportion, precipitation solidifying capacity and simplicity of throwing to attractive shape for an assortment of utilization [1-3]. Al 7075 alloy offers high quality and astounding warm properties among all economically accessible Al alloy and are generally utilized in high focused applications as hang lightweight plane airframes, frame plates, shake climbing apparatus. This amalgam has amazing opposition against fretting wear, fussing exhaustion and crack and utilized in segments such as worm gears which experience such disappointment instruments [4]. One extraordinary utilization of Al 7075 is for making U.S. military M16 rifles and accuracy rifles for the French Arms Company [5]. However, Al 7075 exhibits significant drawbacks in tribological properties due to its high ductility, poor surface hardness and is susceptible to wear [6].

Consequently, much research attention has been given to overcome these drawbacks of Al 7075 through suitable surface modification processes over the past decades. The upgrade of surface mechanical properties for the most part relies upon the level of attachment of layer, which is acquired by fitting Preliminary alloy treatment, preceding coatng [7].Electrical Discharge Machining (EDM) technique, a new recast layer is made on the fabricated external surface. This recast layer includes carbon structures shaped by curve of materials, resulting in restricted solidification and surface flexible stress.

This layer of recasting is verifiably expelled either throu gh hand sprucing or via EDM strategy carving.These layers are alloyed with appropriate particulate powder can satisfactorily increase the texture surface properties and fix lifetime of the components [8].

Few attempts had been made for surface alteration technique for EDM [9] and EDS [10] are detailing somewhere else. The alloying parts like nickel, tungsten, molybdenum, graphite, carbon, silica, and boron and so on were acclimated to advance the peripheral properties. The expansion of the higher than alloying powder improves the mileage obstruction regardless of the texture with self-grease property. A crucial piece of auxiliary materials is surface quality that addresses large surface ends with expanded administration life. A move of surface adjustment structures to strengthen Al alloy's tribological properties. Various covering / alloying strategies are produced with entirely unique mixtures of alloying components as well as their presentations have been assessed by distinct procedures [11]. Of as of late, there is impressive research centre in surface change of Al alloy utilizing electrical discharge alloying (EDA) process, where the device material get stored on the surface of the substrate [12-17]. Stambekova et. al. (2012) analyzed the disintegration and physicochemical features of EDA structured Al 5083 utilizin g unadulterated silicon cathode and extended use impedimen ts owing to alloy[12].In addition, the effect of multiple mach ining parameters on EDA treated with Al 5083 amalgam on hardness and surface brutality was recorded and this examin ation used ferrosilicon anode [13].

Manuscript published on 30 September 2019
***** Correspondence Author
A.Haja Maideen*, Associate Professor, Department of Mechanical Engineering, A.V.C. College of Engineering, Mayiladuthurai, Tamil Nadu 609 305, India,E-mail:hajamaideen2001@gmail.com
Dr. Ing- Muthukannan Duraiselvam, Professor, Department of Production Engineering, National Institute of Technology, Trichy, Tamil Nadu 620 015, India.
Dr. M. Varatharajulu, Department of Mechanical Engineering, A.V.C. College of Engineering, Mayiladuthurai, Tamil Nadu 609 305, India.

Upgraded alloy membrane usage block and nano surface closeness Al4.5FeSi and Al13Fe4 particles are spotted in the alloy layer of Al 5083 made an example of by EDA [14]. The self-lubricated carbon layer was encircled with AA6081 Al-Mg-Si composite using light fuel as a dielectric fluid and discovered that the carbon layer thus created enhanced the electromagnetic impediment ensuring of the amalgam [15]. Scaled down aluminum surface EDA utilizing tungsten anode was tested as well as estimates with unit pits produced in EDA
were also assessed and their volume[16]. Electro discharge alloy of Ti amalgams and the impact on wear control was depicted as the result of the EDA balanced Ti blend surfaces reduced contact coefficient and expanded hardness [17].

Al amalgam surface EDA process includes effective implementation with incredible surface characteristics involves confirmation of most parameters of the appropriate technique. The best approach for coping with different components and their impacts on involvement is accountable for preliminary surface structure [18], which reduces the overall amount of exploratory works likewise as prompts enhancement of a response variable model under.

In this variation, an as of late created strategy, EDA was finished by utilizing an ordinary EDM technique and furthermore the strategy stream mapping is obviously appeared in Fig. 1. Despite the inevitable ongoing EDA process, a white mesh (or) reshuffled layer was shaped to convey carbon heaps from the material curve saved throughout the machined surface to assist obstruction characteristics of hardness and consumption. In this work, Mo in powder kind is utilized to recast with Al combination. Response Surface Methodology (RSM) was utilized for directing the trials and parameter examination was cleared out so as to display the specific wear rate, surface roughness and coefficient of friction [19].

II. EXPERIMENTAL WORK

A. Experimental Procedure

EDA was performed toward one side of Al 7075 round with billet stick of 8 mm width and 30 mm length, which as positive cathode. EDA was done in a self-loader fail horrendously sink EDM invigorated by a 35A heartbeat generator with switch extremity. The common structure of Al 7075 composite is given in Table I. A 200 mm long copper rod as anode has been used as a negative terminal. This strategy was used with a hydrocarbon dielectric medium mixed with Mo powder (50 gm) of 10 to 20 micron atom gage and the blending of Mo powders in the work tank will stop the channel between the essential tank and the work tank, which normally channels the debris surrounded in the middle of the machining [20-21]. To outscore this problem, an exclusively designed machining tank with a flouting point of 10 liters was used for the examination as shown in Fig 2. The multiple parameters of EDA's exploratory methodology suc h as current, waveform and multiple complexities are depict ed elsewhere [22].

Table - I: Chemical composition of Al 7075 Alloy

Element	Mn	Si	Cr	Cu	Fe	Zn	Al	Mg	Ti	Others
Composition (wt.%)	0.3	0.4	0.18 - 0.3	1.2 - 2	0.5	5.1 - 6.1	87 – 90	2.1 - 2.9	0.2	Rest

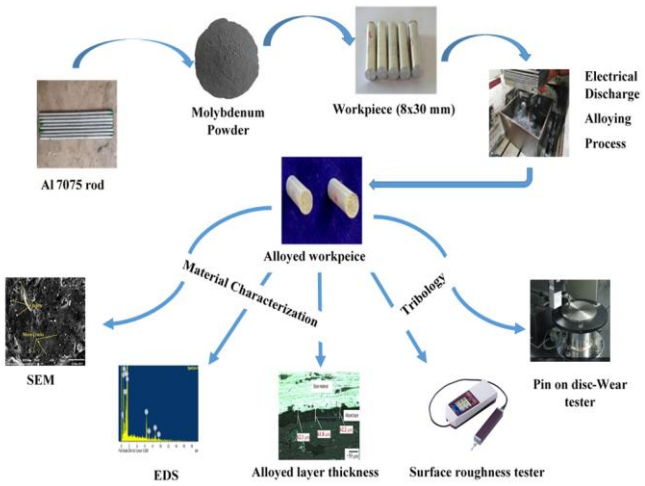

Fig.1. Process flow diagram of electrical discharge alloying

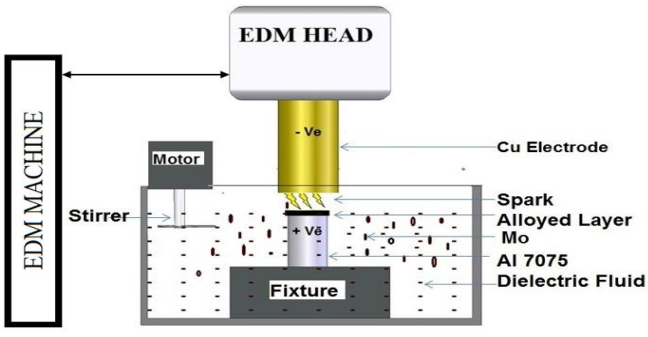

Fig. 2. Schematic view of EDA process

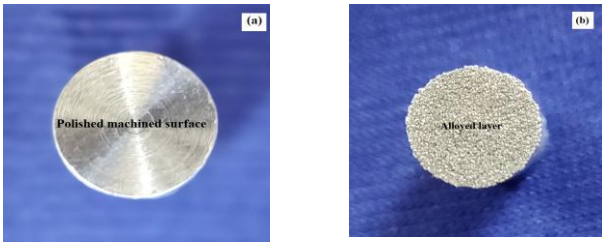

Fig. 3. (a) Machined Surface of Al 7075 work piece and (b) Alloyed Sample Piece

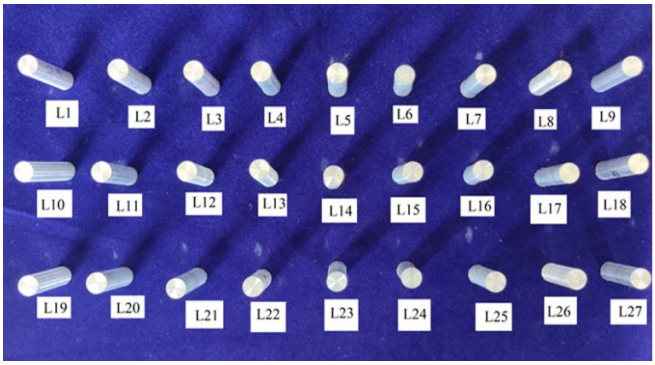

Fig. 4. Alloyed work pieces of Al 7075

The work piece is appeared in the Fig. 3a with fine cleaning surface is engraved to have a uniform structure with no deviations. The alloyed surface is appeared in the Fig. 3.b pinpoint the uniform alloying all through its surface. Fig. 4 demonstrates the structure of alloyed work pieces from experimentation analysis which shows superior alloyed texture in each sample.

On the cross separated bit of alloyed layer, the basic and little auxiliary examination of a alloyed coating was investigated. The samples were installed and very surprising evaluations of mineral sheet size fluctuated from 60 to 1200 microns of coarseness performed by corundum and diamond sprucing were refined. The refined examples was carven for few moments with Krolls etchant to examine the alloyed structure.

B. Wear Test - Pin on Disc Apparatus

Tribometer- Pin on disc, Model (DUCOM), TR-20M-106, has been used to predict the specific wear rate and alloy layer friction coefficient as per ASTM G99-05 standard. As a partner (disc) the sample (alloyed) was drawn as a pin and tempered 10 mm stainless steel round plate. Dry sliding wear experiments were conducted on the alloyed substrate membrane to loads ranging from 5 to 30 N with sliding speeds of 1 to 2 m / s for a continuous sliding departure of 500 m. The wear depth was legitimately determined in the tribometer by the linear differential variable transducer. The fundamental and weight decrease of the tried sample was estimated using deeply accurate electronic gauging machine with objectives of approximately 0.0001 mg. Explicit wear rate was resolved dependent on weight reduction utilizing condition 1 [23].

$$\text{Specific Wear Rate} = \frac{V_L}{L \times SD} \ \text{mm}^3/\text{N-m} \quad (1)$$

Where,

V_L is volume loss in mm^3,
L is load applied in N and
SD is sliding distance in m.

C. Design of Experiment

RSM was utilized to build up the scientific model and to distinguish the impact of the procedure input parameters of the different reactions. In this examination, the test structure was linked to the investigation of the entry variables of the procedure on Peak current (A), P_{on} and P_{off}. L27 symmetrical cluster is used to structure its assessment and Variance Analysis (ANOVA) was implemented using master plan programming. The level of commitment, cooperation and fundamental impacts of control parameters were investigated for different reactions for explicit wear rate, surface roughness and Coefficient of Friction (COF). The variables and its dimensions are definite in Table II.

Table - II: Factors and their levels

Factors / Levels	Unit	Process Parameters		
Peak current	A	6	8	10
P_{on}	µs	100	200	400
P_{off}	µs	150	200	400

III. RESULTS AND DISCUSSION

A. Surface Topography - Alloyed Layer

Fig. 5 demonstrates the optical minuscule picture of the alloyed sample and alloyed layer thickness ranges between 60-63 µm which were observed to be most extreme at pinnacle current of 8 amps, 200 µs P_{on} and 150 µs P_{off}. A distinctive uniform structure of alloyed layer was seen with thickness running of close-by esteems showed alongside base metal [22].

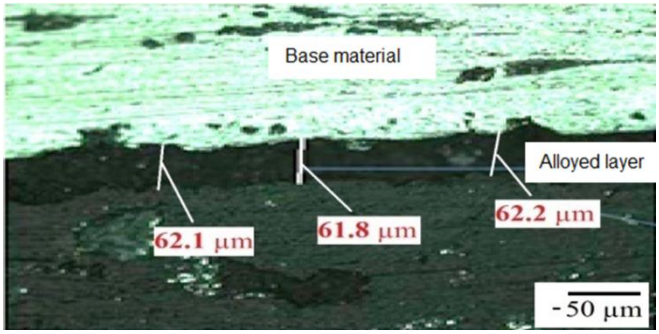

Fig. 5 Optical microscope view of alloyed layer thickness

Fig. 6 (a, b, c and d) represents SEM pictures of alloyed examples at various procedure parameters on top alloyed surface of Al 7075. Fig. 6 (a, b) reveals better attachment of covering captured superficially. The alloyed sample affirms the nearness of Mo and surface was without voids, blowholes and small scale splits. The non-appearance of real deformities enrolled above uncovers that alloyed surface has superb metallurgical holding joined with basic homogeneity.

Fig. 6 (c, d) demonstrates the SEM picture with better alloyed surface with negligible splits noted. The components such as C, O, Mg, Al, Zn, L, W, M with fortified Mo was seen alongside base metal is clearly encroached from EDXA investigation as appeared in Fig. 7. The bead event as combined carbon is recipient in EDA procedure and goes about as a self-oil. The weight rates of every component on the alloyed layer are recorded in.Fig.8

The nearness of Mo has been affirmed by SEM and EDXA examination as low as 0.13 wt. % because of disintegration of terminal and low level of Mo powder suspended in the dielectric liquid.

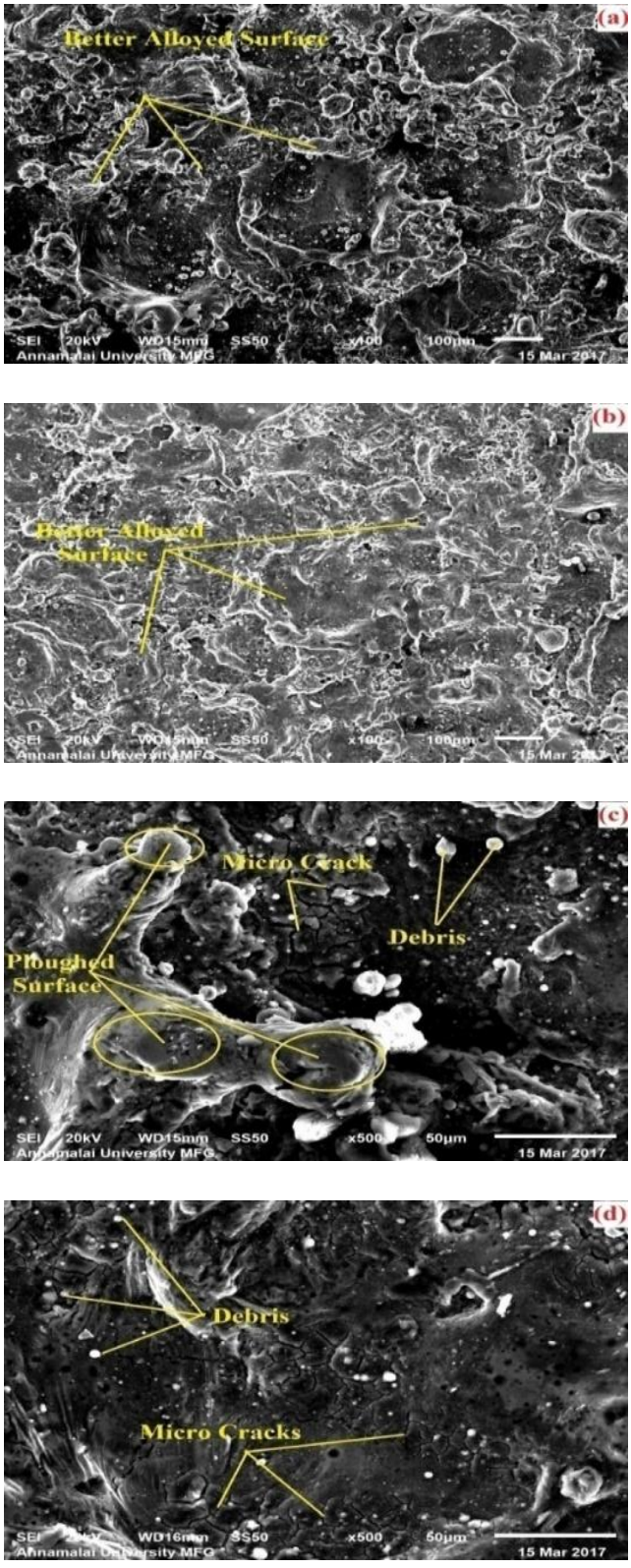

Fig. 6. SEM image on (a & b) uniform alloyed surface, (c) carbon flakes and (d) better alloyed surface (8 A, 200 µs P_{on} and 150 µs P_{off})

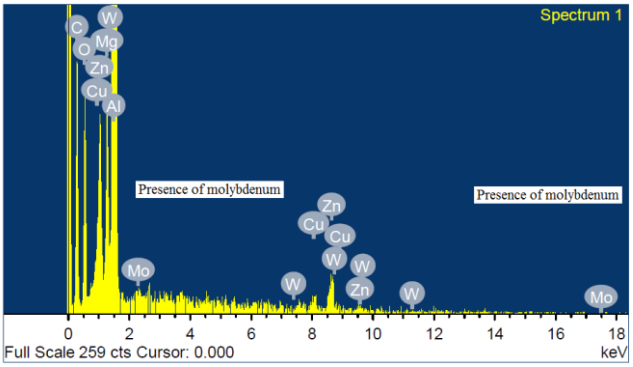

Fig. 7. EDS spectrum of alloyed sample

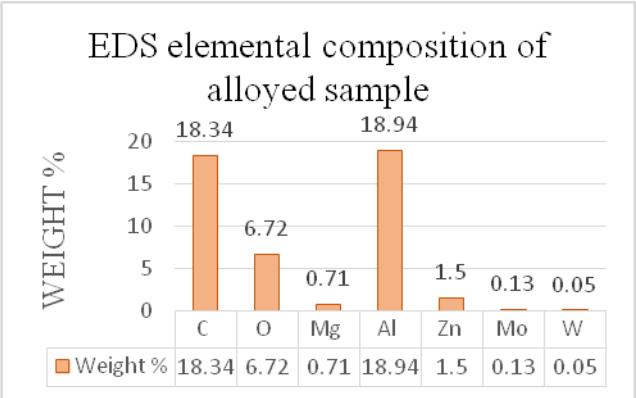

Fig. 8. EDS composition of alloyed sample

When all is said in done, the splits were framed essentially because of high warm pressure prompted by high pinnacle current and cooling at a quicker rate. The break proliferation was observed to be insignificant, due to Mo, which hinders the design of carbon underneath the alloyed layer and furthermore in the heat influenced zone.

B. Specific Wear Rate

The particular wear rate of alloyed surface appeared in Fig. 9(a) penlights better wear obstruction when compared with that of base material. The alloyed layer of the material has magnificent warm strength and the particular wear rate saw to be low at lower current, where by at greatest current, it will in general increment. The event of tolerably softened Mo from EDXA investigation bear higher rough wear obstruction and will in general strip off. As effective coating of this delicate layer, the carbides development bears the greatest protection from plastic distortion. Besides, this kind of alloyed layer the opposition essentially follow upon the presence of the components that lessen the fragile idea of the carbon. By full wear test, the withstanding limit of the coating can be found.

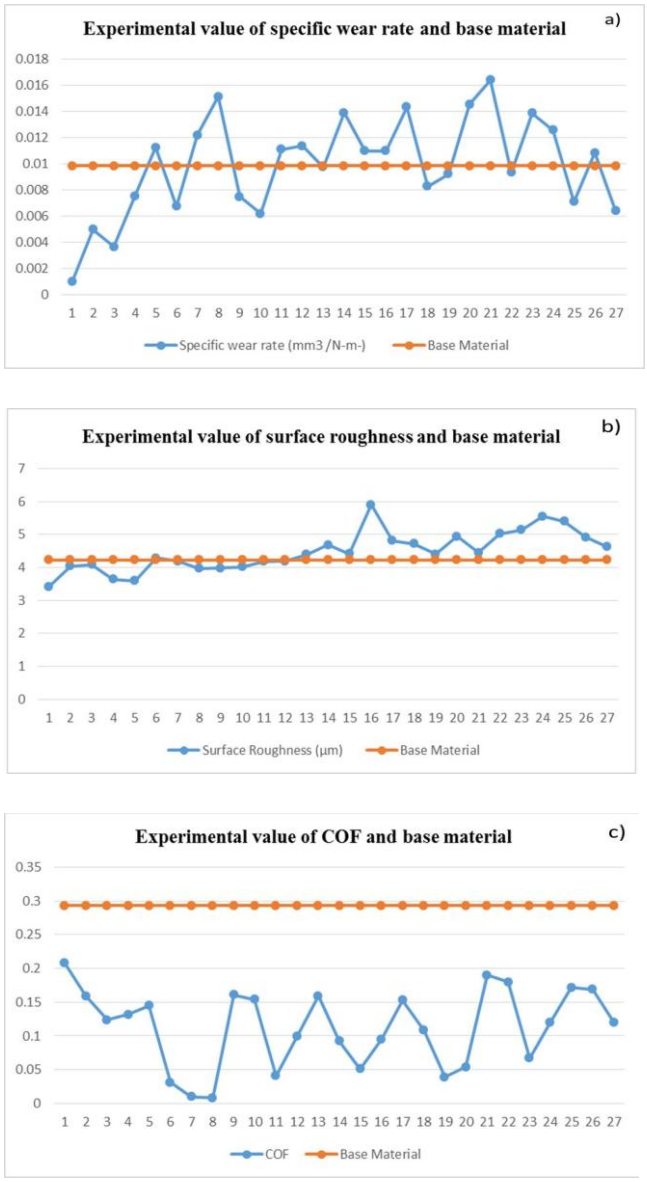

Fig. 9 (a). Experimental value of specific wear rate with base metal, (b) Experimental value of surface roughness with base metal and (c) Experimental value of coefficient of friction with base metal

In the range of 0.0009696 and 0.164038 mm3/N-m the specific wear frequency of Al 7075 alloyed with Mo differs. The highest specific wear frequency of the stick was 0.164038 mm3/N-m at 10 amps pinnacle current with P_{on} and P_{off} moment as 100 and 400 µs separately.By utilizing the test plan, the best procedure parameter was recognized as 6 amps pinnacle current, 100 µs P_{on} and 150 µs P_{off}. Utilizing this ideal parameter, explicit wear rate of alloyed layer was limited to a conceivable degree for EDA test.

C. Surface Roughness

The surface unpleasantness of both alloyed surface and base material is appeared in Fig 9 (b) disavows better surface roughness. It was seen that the normal surface discomfort of alloyed material was 1.05 times less than that of the base material. The alloyed layer's surface roughness varies between 3,426 and 5,895 µm. It was seen that the most extreme surface roughness acquired when the pinnacle current was 8 amps, P_{on} as 400 µs and P_{off} as 150 µs. The base surface roughness of 3.426 µm with 6 amps pinnacle current, P_{on} and P_{off} of 100 and 150 µs was seen that demonstrates lesser amps with ostensible P_{on} and P_{off} is best for getting better surface roughness[24-25].

D. Coefficient of Friction

It demonstrates the connection between the frictional powers sandwiched between two objects. The alloyed layer friction coefficient at various parameters was registered in the. Fig. 9 (c) demonstrates lesser esteem values when contrasted and that of base metal. The trial esteem for COF of the alloyed layer recorded by the wear testing machine ranges from 0.008-0.208. As the esteem is not as much as solidarity the opposing power is inside the farthest point shows more secure esteem and it tends to be taken into examination for some building applications.

Wear method involves three overwhelming dynamic phases at different stacking circumstances (I) delamination, (ii) ploughing, and (iii) oxidation [22].The well-used surfaces and the delaminated layer were obviously encroached in the SEM picture appeared in the Fig 10 (a, b and c). A reasonable edge of delaminated surface layer, shallow heads and small scale splits penlights in Fig 10 (a, b). Delaminated layer alongside a little pit, permeable and little cleavages were seen in Fig 10 (c). At high burden, as temperature expands, the periphery (delaminated) layer bit by bit reduced. In the alloyed surface, the pinnacles and valleys became soft and delicate, resulting in a greater wear rate with less friction coefficient [26]. Ploughing is the following phase of delamination, because of garbage and amid sliding. The ploughing groove was nearly reduced at higher temperature, which prompts the fall in the surface roughness esteems. The following stage is oxidation because of natural response between the wear samples. The oxidation typically saw between the contact surfaces.

By and large, at higher temperature the alloyed surface get delicate, results in self-grease properties. The fundamental element present such as C, O, Mg, Zn, and K alongside base metal Al appeared in Fig. 11 and the weight rates after wear test appeared in the histogram diagram in Fig 12.

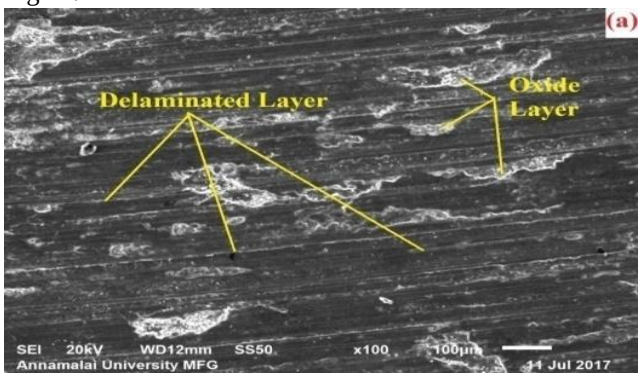

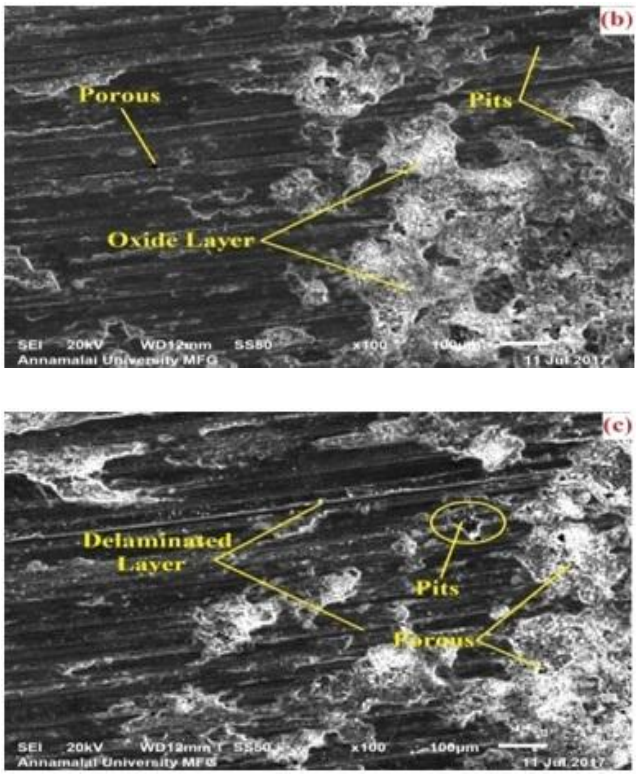

Fig. 10. (a, b &c) SEM images after wear test using pin on disc

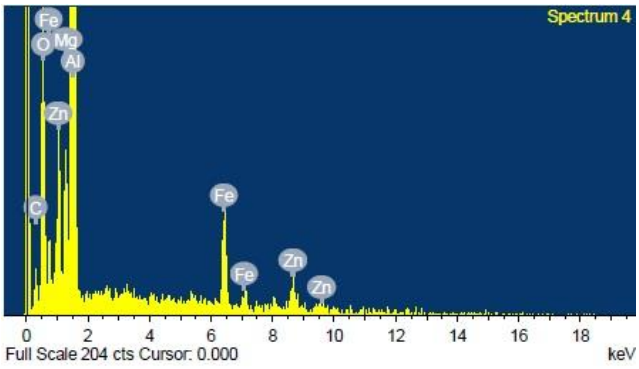

Fig.11. EDS spectrum of alloyed sample after wear test

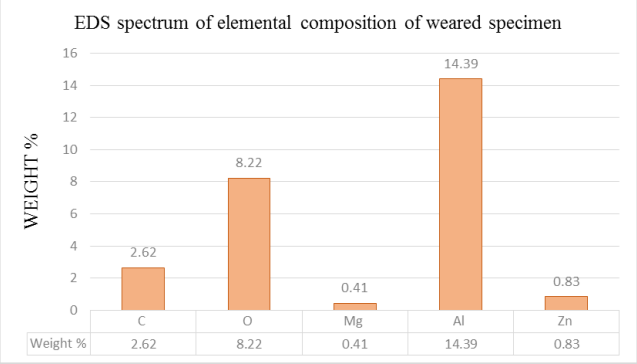

Fig. 12. EDS composition of weared sample

E. ANOVA with Response Plots

The ANOVA was used to explore the impact of information parameters on reaction factors [27]. Tables III, IV, V provide the ANOVA outcomes separately for the particular wear rate, surface roughness and COF. ANOVA was also used to aggregate the significance test for individual model coefficient. The F-esteem (Model) of 2900 in Table III demonstrates that the model terms were significant. Estimations of "Prob > F" under 0.05 infers that the model terms were critical. For this situation, the terms A, B, AB, AC, BC, A^2, B^2, C^2, AB^2, B^2C are critical model terms. As qualities are higher than 0.05 it suggests the model terms were not noteworthy. The "Pred R-Squared" of 0.9980 was in practical concurrence with the "Adj R-Squared" of 0.9994. The typical lingering plot diagram for explicit wear rate is appeared in the Fig. 13 (a), uncovers the closeness of level of ordinary likelihood, effectively utilized for further examination.

The collaboration between the data sources (P_{on} and Peak current) and yield reaction of explicit wear rate is appeared in the Fig. 13 (b). The impact of pinnacle current over the particular wear rate was discovered insignificant amid P_{on}, discontinuous and higher range. Bigger the current, bigger is the particular wear rate while P_{on} in lower go. Higher the P_{on}, higher is the particular wear rate on account of lower current. Increment in P_{on}, expands the particular wear rate in the irregular range.

The combined effect of lower P_{on} and higher current produces more specific wear rate. Also the combined effect of lower P_{on} and lesser current generates smaller specific wear rate. The interaction between the inputs (P_{off} & current) and output response of specific wear rate is detailed in Fig. 13 (c). At higher current, it has less influence over specific wear rate. In the intermittent range and low range of current the specific wear rate was found neglible when compared P_{off}. Higher the P_{off}, the specific wear rate was found to be low and in the intermittent range it rapidly increases to its maximum position. In lower P_{off}, the influence of specific wear rate was found to be in intermittent range when compared with current. The combined effect of intermittent P_{off} and higher current produces more specific wear rate. Also the combined effect of higher P_{off} and lesser current generates smaller specific wear rate.

Table - III: ANOVA Table for Specific wear rate

Source	Sum of Squares	DF	Mean Square	F Value	p-value Prob> F
Model	3.65E-04	16	2.28E-05	2.90E+03	**< 0.0001**
A-Current	7.90E-07	1	7.90E-07	1.00E+02	< 0.0001
B-Pulse on	4.21E-07	1	4.21E-07	5.34E+01	< 0.0001
C-Pulse off	2.72E-08	1	2.72E-08	3.45E+00	0.093
AB	1.34E-04	1	1.34E-04	1.69E+04	< 0.0001
AC	1.28E-05	1	1.28E-05	1.62E+03	< 0.0001
BC	4.51E-05	1	4.51E-05	5.73E+03	< 0.0001
A^2	9.75E-06	1	9.75E-06	1.24E+03	< 0.0001
B^2	9.03E-06	1	9.03E-06	1.15E+03	< 0.0001
C^2	7.80E-05	1	7.80E-05	9.90E+03	< 0.0001
ABC	1.36E-08	1	1.36E-08	1.73E+00	0.2183

A^2B	5.30E-09	1	5.30E-09	0.67	0.4313
A^2C	3.97E-09	1	3.97E-09	0.5	0.4941
AB^2	4.63E-06	1	4.63E-06	5.88E+02	< 0.0001
AC^2	1.59E-08	1	1.59E-08	2.01	0.1863
B^2C	1.65E-06	1	1.65E-06	2.10E+02	< 0.0001
BC^2	1.21E-08	1	1.21E-08	1.53	0.2437
Residual	7.88E-08	10	7.88E-09		
Cor Total	3.65E-04	26			

Table - IV: ANOVA Table for Surface Roughness

Source	Sum of Squares	DF	Mean Square	F Value	p-value Prob> F
Model	8.9	16	0.56	13.17	**0.0001**
A-Current	0.83	1	0.83	19.55	0.0013
B-Pulse on	1.77E-03	1	1.77E-03	0.042	0.842
C-Pulse off	1.19E-03	1	1.19E-03	0.028	0.8698
AB	0.025	1	0.025	0.58	0.4627
AC	0.14	1	0.14	3.25	0.1014
BC	0.76	1	0.76	18.11	0.0017
A^2	0.16	1	0.16	3.77	0.081
B^2	0.22	1	0.22	5.26	0.0448
C^2	0.017	1	0.017	0.41	0.5375
ABC	8.82E-05	1	8.82E-05	2.09E-03	0.9644
A^2B	0.61	1	0.61	14.36	0.0035
A^2C	0.18	1	0.18	4.19	0.0679
AB^2	0.33	1	0.33	7.8	0.019
AC^2	9.07E-04	1	9.07E-04	0.021	0.8864
B^2C	0.23	1	0.23	5.54	0.0404
BC^2	0.62	1	0.62	14.69	0.0033
Residual	0.42	10	0.042		
Cor Total	9.32	26			

The interaction between the inputs (P_{on} & P_{off}) and output response of specific wear rate is shown in Fig 13 (d). At higher P_{on}, intermittent P_{on} and low P_{on} it has same influence over specific wear rate in contrast with P_{off}. And in low level of $P_{off,}$ it shows lesser specific wear rate. In the intermittent range of $P_{off,}$ it gradually increases to maximum and in higher P_{off} , it tends to decrease.

Table - V: ANOVA Table for COF

Source	Sum of Squares	DF	Mean Square	F Value	p-value Prob> F
Model	0.077	16	4.80E-03	4.76	**0.0082**
A-Current	1.39E-04	1	1.39E-04	0.14	0.7184
B-Pulse on	4.12E-03	1	4.12E-03	4.08	0.0709
C-Pulse off	0.013	1	0.013	13.11	0.0047
AB	0.01	1	0.01	9.94	0.0103
AC	2.25E-07	1	2.25E-07	2.23E-04	0.9884
BC	8.67E-04	1	8.67E-04	0.86	0.3756
A^2	9.13E-04	1	9.13E-04	0.91	0.3638
B^2	1.71E-03	1	1.71E-03	1.69	0.2223
C^2	2.63E-03	1	2.63E-03	2.61	0.1375
ABC	0.029	1	0.029	28.88	0.0003
A^2B	1.83E-03	1	1.83E-03	1.81	0.2081
A^2C	2.60E-03	1	2.60E-03	2.58	0.1392
AB^2	1.15E-03	1	1.15E-03	1.14	0.3104
AC^2	5.97E-04	1	5.97E-04	0.59	0.4593
B^2C	0.011	1	0.011	11.13	0.0075
BC^2	3.53E-03	1	3.53E-03	3.49	0.0911
Residual	0.01	10	1.01E-03		
Cor Total	0.087	26			

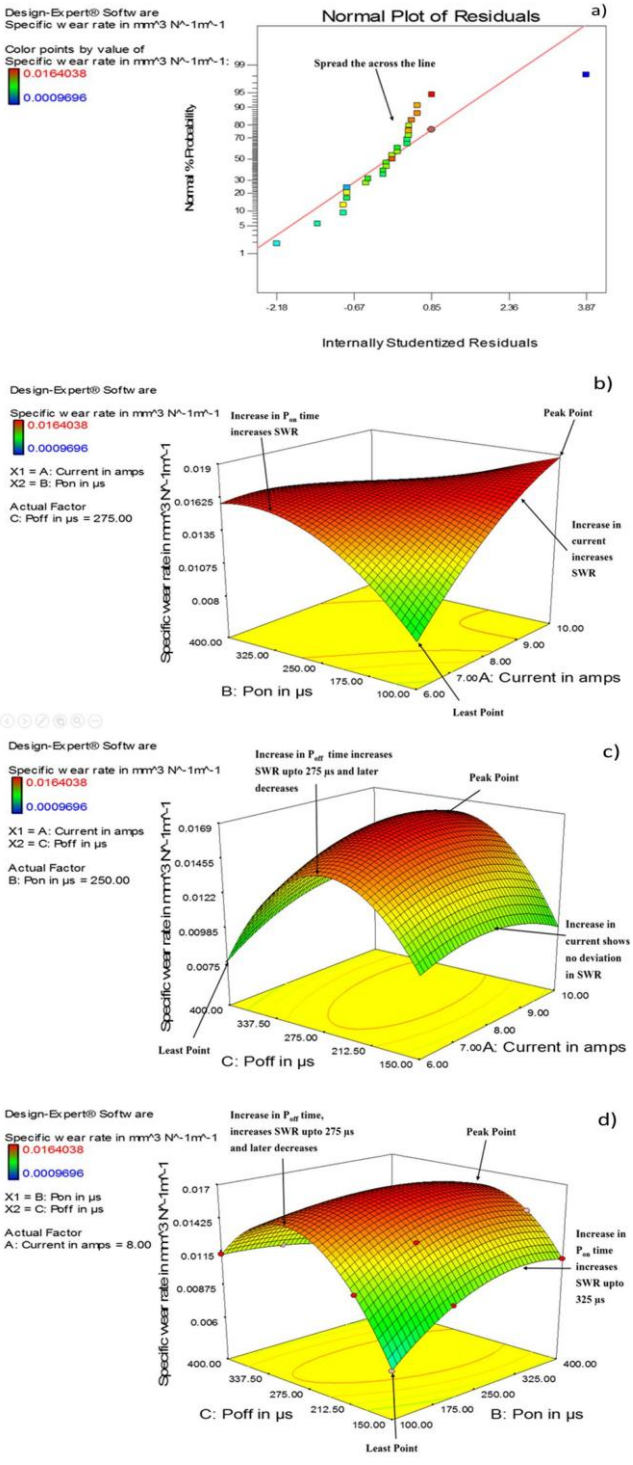

Fig. 13 (a) Normal distribution residual plot of specific wear rate, (b) Response surface effect of current and P_{on} on specific wear rate (c) Response surface effect of current and P_{off} on specific wear rate and (d) Response surface effect of P_{on} and P_{off} on specific wear rate

The combined effect of intermittent P_{off} and current in all mode produces more specific wear rate. Also the combined effect of higher P_{on} and lower P_{off} will result in lesser specific wear rate. The F-value (Model) of 13.17 shows the model is vital. The normal residual plot graph for surface roughness shown in Fig. 14 (a), reveals the closeness of percentage of normal probability and can be successfully employed for further examination.

The interaction between the inputs (P_{on} & Current) and output response of surface roughness is shown in the Fig. 14 (b). At high current, it has more influence over surface roughness (increases) when compared with P_{on}. In the intermittent range of current, it gradually shows reduced value of surface roughness. In comparison to P_{on}, surface roughness was revealed to be very small at low current. At elevated P_{on}, the surface roughness was discovered to be small and tends to increase in the intermittent spectrum.. At low level of P_{on} there was a dramatic change in surface roughness i.e. gradually increases. At lesser P_{on} with lesser current, surface roughness values found to be high. The combined effect of lower P_{on} and higher Current produces more surface roughness. Also the combined effect of higher P_{on} and lesser current generates smaller surface roughness.

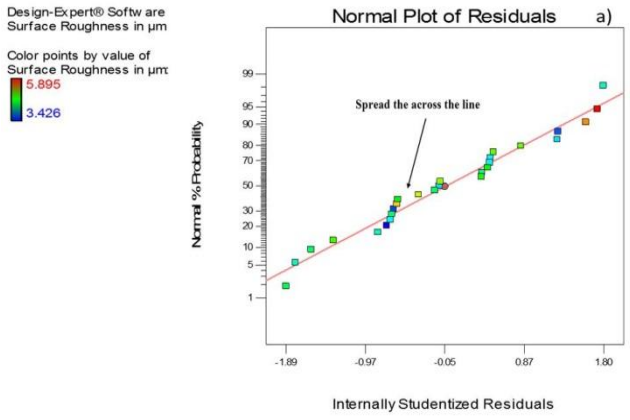

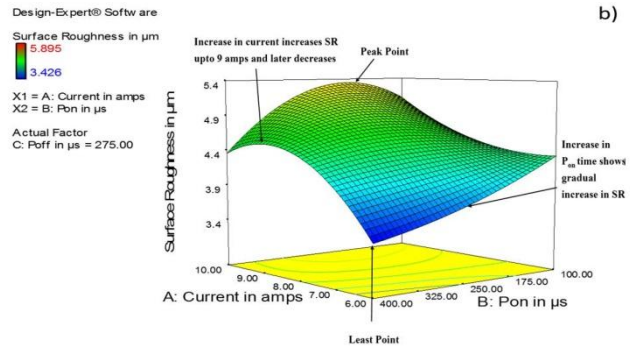

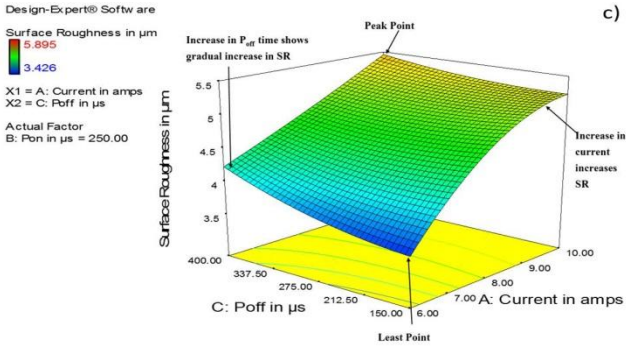

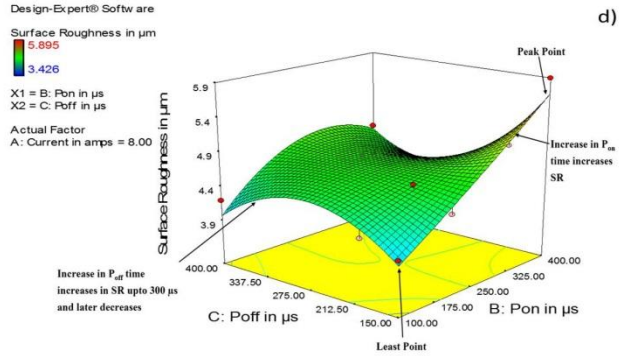

Fig. 14. (a) Normal distribution residual plot of surface roughness, (b) Response surface effect of current and P_{on} on surface roughness, (c) Response surface effect of current and P_{off} on surface roughness and (d) Response surface effect of P_{on} and P_{off} on surface roughness

The interaction between the inputs (P_{off} & Current) and output response of surface roughness is shown in the Fig. 14 (c). At high current, more surface roughness value was shown due to generation of high temperature. In the intermittent range of current, the surface roughness gradually decreases. In low level of current, it has minimum surface roughness due to smooth surface impringed on alloyed layer. In P_{off}, it has same influence in all modes of surface roughness, in contrast with current.

The interaction between the inputs (P_{on} & P_{off}) and output response of surface roughness is shown in the Fig. 14 (d). At higher P_{on}, it shows higher surface roughness value and in the intermittent range the surface roughness value tends to increase nominally. At low P_{on}, it has less influence over surface roughness. Whereas at low level of $P_{off,}$ it shows merely lesser surface roughness and tends to increase in intermittent range. In high P_{off}, it results in lesser surface roughness value. The normal residual plot graph for coefficient of friction is shown in Fig. 15 (a), reveals the closeness of percentage of normal probability and can be successfully employed for further examination.

The interaction between the inputs (P_{on} & Current) and output response of COF is shown in Fig. 15 (b) At high P_{on}, it has more influence over COF (increases) when compared with P_{on}. In the intermittent range of $P_{on,}$ it has same impact and gradually increases in low P_{on}. At high Current, the COF was found to be low and then gradually increased in the intermittent value.At low current, COF has more impact and have higher values.

The combined effect of lower P_{on} and higher current produces less COF. Also the combined effect of higher P_{on} and higher current genarates higher COF. The interaction between the inputs (P_{off} & Current) and output response of COF is shown in the Fig. 15(c). At higher current, it shows rapid increase in COF in contrast with P_{off}. In the intermittent range of current the COF gradually decreases. In low level of current it shows gradual decrease when compared with P_{off}. In high P_{off}, it shows minimum COF value and gradually increased and vice- versa in low P_{off}. The combined effect of lower P_{off} and higher current shows more COF. Also the combined effect of higher P_{off} and lesser current generates lesser COF values.

The interaction between the inputs (P_{on} & P_{off}) and output response of SR is shown in the Fig. 15 (d). At high P_{on}, SR value has more impact and high in the intermittent range. And in low level of $P_{on,}$ shows merely greater COF. In low $P_{off,}$ it has greater impact of COF at higher value and in intermittent it tends to decrease and in high $P_{off,}$ it merely shows increased COF value.

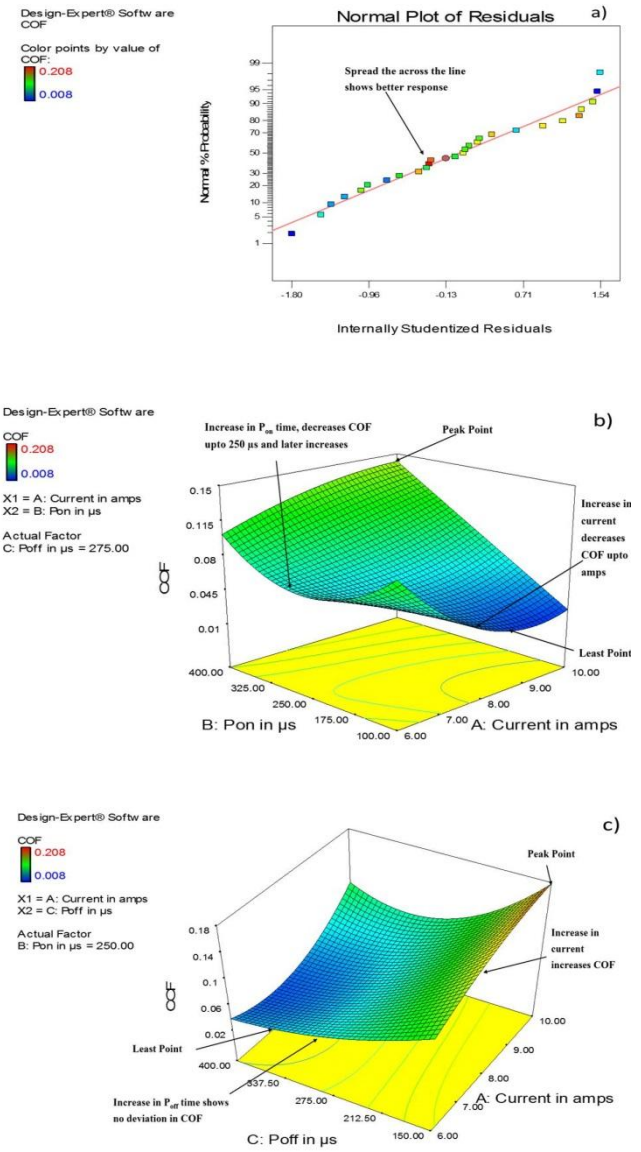

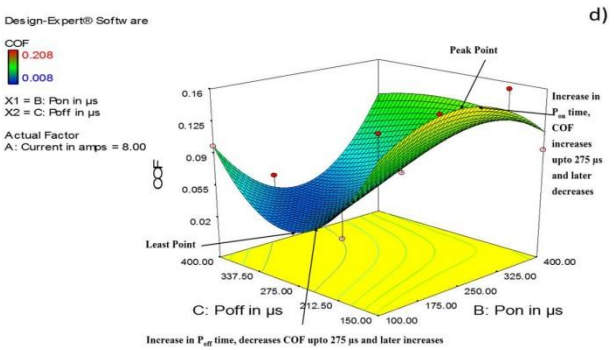

Fig. 15 (a) Normal distribution residual plot of COF, (b) Response surface effect of current and P_{on} on COF, (c) Response surface effect of current and P_{off} on COF and (d) Response surface effect of P_{on} and P_{off} on COF

F. Statistical Model

Table - VI: Regression Analysis

Statistical values	Specific Wear Rate	Surface Roughness	COF
R-Squared	0.9998	0.954705	0.883968
Adj. R-Squared	0.9994	0.882232	0.698317
Pred. R-Squared	0.998	0.590109	0.156639
Adeq. Precision	2.21E+02	13.461	9.023264

The regression models of specific wear rate, surface roughness and COF were presented in the equation 2, 3 and 4 respectively [28]. Table VI shows the regression statistics and coefficient of determination values closer to unity holds good reliability, therefore the model can be taken for further analysis. The uncontrollable factors are accounted by Adeq. Precision. In the present study, it seems to be good because the output response have greater value than four.

G. Assessment of Regression Analysis

Appraisal of response condition is mandatory to characterize the consistency. The consequences of anticipated explicit wear rate, surface roughness and COF was in great concurrence with the test information. The Table VII demonstrates the examination between real (analyze) versus predicted (got from numerical model) reactions and level of deviation between genuine versus anticipated qualities. The distinction between the real and the anticipated qualities are nearer to it and utilized for further examinations. The normal level of deviation for explicit wear rate was noted as 1.960, surface roughness as 2.374 and COF was determined as 19.063.

$$\text{Specific Wear Rate} = -0.074573 + 8.24022\times10^{-3}\times A + 2.89705\times10^{-4}\times B - 1.93208\times10^{-4}\times C - 2.38711\times10^{-5}\times A\times B + 7.19839\times10^{-6}\times A\times C - 1.97821\times10^{-7}\times B\times C - 2.98582\times10^{-4}\times A^2 - 3.51383\times10^{-7}\times B^2 - 3.4869\times10^{-7}\times C^2 - 1.02015\times10^{-9}\times A\times B\times C - 5.95625\times10^{-8}\times A^2\times B - 5.95298\times10^{-8}\times A^2\times C + 2.74026\times10^{-8}\times A\times B^2 - 3.332501\times10^{-9}\times A\times C^2 + 2.47463\times10^{-10}\times B^2\times C - 3.80929\times10^{-11}\times B\times C^2 \quad (2)$$

$$\text{Surface Roughness} = +1.00779 - 0.18426\times A - 0.054696\times B + 0.057594\times C + 0.013976\times A\times B - 6.36986\times10^{-3}\times A\times C - 1.17607\times10^{-4}\times B\times C + 7.89286\times10^{-3}\times A^2 - 0.23\times10^{-3}\times B^2 + 7.39504\times10^{-5}\times C^2 - 5.61033\times10^{-5}\times A\times B\times C + 8.21429\times10^{-8}\times A^2\times B + 3.97262\times10^{-4}\times A^2\times C - 7.30278\times10^{-6}\times A\times B^2 - 7.96667\times10^{-7}\times A\times C^2 - 9.30238\times10^{-8}\times B^2\times C + 2.72776\times10^{-7}\times B\times C^2 \quad (3)$$

$$\text{Coefficient of friction} = +1.13041 - 0.079258\times A - 7.02759\times10^{-3}\times B - 4.55056\times10^{-4}\times C + 1.28489\times10^{-3}\times A\times B - 7.54369\times10^{-4}\times A\times C + 1.35147\times10^{-3}\ B\times C + 1.35147\times10^{-3}\times A^2 - 1.26944\times10^{-6}\times B^2 + 2.20333\times10^{-6}\times C^2 - 1.49311\times10^{-6}\times A\times B\times C - 3.49702\times10^{-5}\times A^2\times B + 4.82143\times10^{-5}\times A^2\times C - 4.31944\times10^{-7}\times A\times B^2 + 6.46667\times10^{-4}\ A\times C^2 + 2.03889\times10^{-8}\times B^2\times C - 2.0566\times10^{-8}\times B\times C^2 \quad (4)$$

The Fig 16 (a, b & c) indicates the actual and predicted comparison plot for specific wear rate, surface roughness and COF respectively. The actual values were very closer to predicted values particular for the lower specific wear rate and nominal range of surface roughness throughout its trail run and also for COF. From this investigation, the results were in close concurrence with experimental value from the experimental design and effectively used to examine the influence of process parameter over responses in alloying of Al 7075 with Mo powder.

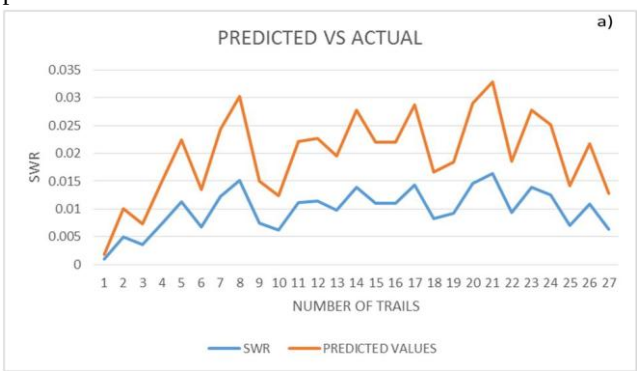

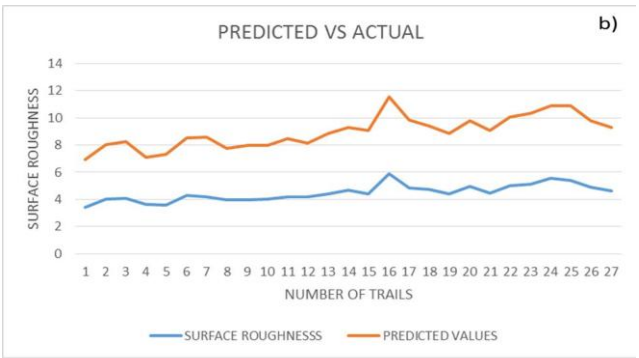

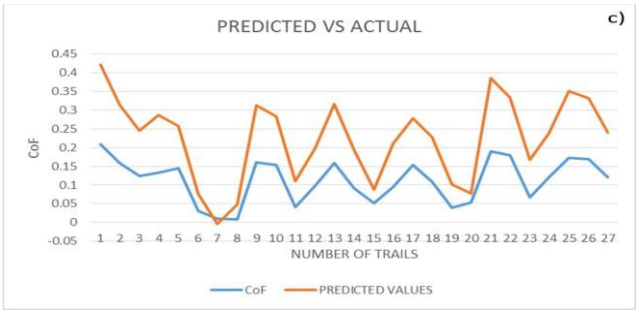

Fig. 16 (a) Actual Vs Predicted Specific Wear Rate, (b) Actual Vs Predicted Surface Roughness and (c) Actual Vs Predicted COF.

Table - VII: Actual versus predicted Specific wear rate, Surface roughness and Coefficient of friction and it's percentage of deviation

Expt. No	Actual Specific wear rate	Predicted Specific wear rate	% of deviation	Actual Surface Roughness	Predicted Surface Roughness	% of deviation	Actual COF	Predicted COF	% of deviation
1	0.000969	0.000812	16.2	3.426	3.509481	2.44	0.208	0.213539	2.66
2	0.004994	0.00511	2.32	4.035	3.973098	1.53	0.159	0.154702	2.70
3	0.003658	0.003677	0.50	4.086	4.147279	1.50	0.124	0.120688	2.67
4	0.007495	0.007605	1.46	3.646	3.474636	4.70	0.132	0.153799	16.5
5	0.011230	0.011188	0.38	3.598	3.690505	2.57	0.145	0.112334	22.5
6	0.006734	0.006704	0.46	4.283	4.237574	1.06	0.031	0.044974	45.0
7	0.012184	0.012201	0.13	4.194	4.375756	4.33	0.01	-0.01385	38.4
8	0.015128	0.015095	0.22	3.965	3.817057	3.73	0.008	0.040599	7.49
9	0.007473	0.00556	25.6	3.986	3.993616	0.19	0.161	0.151211	6.08
10	0.006175	0.006268	1.50	4.019	3.951608	1.68	0.154	0.128857	16.3
11	0.011100	0.011076	0.22	4.182	4.307344	3.00	0.041	0.069786	70.2
12	0.011368	0.011348	0.18	4.194	3.970334	5.33	0.099	0.0995	0.51
13	0.009746	0.009734	0.13	4.387	4.492596	2.41	0.159	0.157468	0.96
14	0.013881	0.013816	0.47	4.679	4.601405	1.66	0.092	0.100837	9.61
15	0.010989	0.010996	0.06	4.42	4.64057	4.99	0.051	0.03748	26.5
16	0.010979	0.010963	0.15	5.895	5.66905	3.83	0.095	0.11469	20.7
17	0.014325	0.014337	0.08	4.818	5.004934	3.88	0.153	0.124107	18.8
18	0.008273	0.008302	0.36	4.724	4.680159	0.93	0.108	0.119274	10.4
19	0.009206	0.009217	0.11	4.405	4.423973	0.43	0.039	0.063461	62.7
20	0.014532	0.01451	0.16	4.938	4.830732	2.17	0.054	0.023441	56.5
21	0.016403	0.016392	0.07	4.447	4.618152	3.85	0.19	0.194026	2.12
22	0.009322	0.009307	0.16	5.018	5.031176	0.26	0.18	0.152447	15.3
23	0.013858	0.013865	0.05	5.141	5.19183	0.99	0.067	0.099936	49.1
24	0.012569	0.012615	0.36	5.547	5.358709	3.39	0.12	0.117725	1.90
25	0.007100	0.007074	0.38	5.402	5.463724	1.14	0.172	0.178584	3.83
26	0.010847	0.010903	0.52	4.914	4.853096	1.24	0.169	0.162258	3.99
27	0.006398	0.006357	0.65	4.622	4.662608	0.88	0.12	0.119122	0.73

H. Confirmation Test

The confirmation test was performed with the desired parameters which produces minimized specific wear rate and surface roughness. The specimen was alloyed with best optimal parameter of 6 amp peak current with P_{on} and P_{off} of 100 µs and 150 µs for surface roughness. The specific wear rate was found to be better at than other parameters 6 amp peak current with P_{on} and P_{off} of 100 µs and 150 µs respectively.

IV. CONCLUSIONS

EDA was effectively performed over the surface of Al 7075 with Mo powder and exposed to wear test. Explicit wear rate, surface harshness and COF were explored with the assistance of RSM investigation. The outcomes were examined utilizing MINITAB 16. In view of the outcomes, following ends were made.

- The alloyed layer thickness was observed to be uniform in all through its structure with great holding.
- The SEM investigation affirmed the nearness of Mo alongside the grain limits shows uniform dispersion on alloyed surfaces.
- The alloyed layer thickness was found to be uniform in most of the parameter setting.
- From the main effect plot, the optimum level for minimum specific wear rate was identified as 6 amps current, 100 µs P_{on} and 150 µs P_{off} .
- From the main effect plot, the optimum level for minimum surface roughness was identified as 6 amps Current, 100 µs P_{on} and 150 µs P_{off}.
- Significant process parameters were identified using ANOVA.
- The influence of independent variable over dependable were examined using 3D surface plots.
- P_{off} time is more responsible for perfect coating of material in EDA and also responsible for providing crack free surface with minimum specific wear rate and roughness.
- EDA has improved the wear resistance and minimized surface roughness when compared to the base material.

REFERENCES

1. S. Bera, S.G. Chowdhury, Y. Estrin and I.Manna " Mechanical properties of Al7075 alloy with nano-ceramic oxide dispersion synthesized by mechanical milling and consolidated by equal channel angular pressing", Journal of Alloys and Compounds,548, 257-65 (2013)
2. M.S.Kenevisi and S.M,Mousavi Khoie, "An investigation on microstructure and mechanical properties of Al7075 to Ti–6Al–4V Transient Liquid Phase (TLP) bonded joint", Materials & Design,38,19-25 (2012)
3. N. Yazdian, F. Karimzadeh and M. Tavoosi,, "Microstructural evolution of nanostructure 7075 aluminum alloy during isothermal annealing", Journal of Alloys and Compounds,493(1–2), 137-141(2010)
4. E. Mohseni, E. Zalnezhad, Ahmed A. D. Sarhan and A. R. Bushroa. "Achievements in engineering materials, energy, management and control based on information technology", Pts 1 and 2, Article ID 474723, 17 pages (2014)
5. P. John and R.Davis, "Performance study of electrical discharge machining process in burr removal of drilled holes in Al 7075", Cogent Engineering. 3:1-19 (2016)
6. A.Baradeswaran, S C. Vettivel, A E.Perumal, N. Selvakumar and R F.Issac, "Experimental investigation on mechanical behaviour, modelling and optimization of wear parameters of B4C and graphite reinforced aluminium hybrid composites", Materials &. Design. 63:620-632 (2014)

7. J.Sudagar, K.Venkateswarlu and J.Lian, “Dry sliding wear properties of a 7075-T6 aluminum alloy coated with Ni-P (h) in different pretreatment conditions”, Journal of Materials Engineering and Performance. 19(6): 810-818 (2010)
8. S. Chakraborty, S. Kar, V.Dey and S. Ghosh, “The Phenomenon of Surface Modification by Electro-Discharge Coating Process: A Review”, Surface Review and Letters 25(1):389 (2018)
9. S.Kumar, R.Singh and T P. Singh, “Comparison of material transfer in electrical discharge machining of AISI H13 die steel”, Journal of Materials Processing Technology. 223(7):1733-1740 (2009)
10. S Y.Chang, H S.Jang, Y H.Yoon,“Self-Consolidation and Surface Modification of Mechanical Alloyed Ti-25.0 at.% Al Powder Mixture by Using an Electro-Discharge Technique”, Archives of Metallurgy and Materials. 62(2B):1293-1297 (2017).
11. I S.Batra, K. Bhanumurthy and S K.Khera, “Surface alloying of pure iron by molybdenum and tin by a continuous wave CO_2 laser”, Bulletin of Materials Science. 16(5):331-340 (1993).
12. K Stambekova, H M Lin and J Y. Uan, “Microstructural and corrosion characteristics of alloying modified Layer on 5083 Al alloy by electrical discharge alloying process with pure silicon electrode”, Materials Transactions. 53(8):1436-1442 (2012)
13. H M.Lin, S.Kuralay and J Y.Uan, “Microstructural and corrosion characteristics of iron-silicon alloyed layer on 5083 Al alloy by electrical discharge alloying processing”, Materials Transactions. 52(3):514-520 (2011)
14. K.Stambekova, H M Lin,and J Y Uan , “Surface modification of 5083 Al alloy by electrical discharge alloying processing with a 75 mass% Si–Fe alloy electrode”, Applied Surface Science 258(10): 4483-4488 (2012).
15. Wang-Chih CHEN, Hung-Mao LIN and Jun-Yen UAN, “Formation and characterization of self-lubricated carbide layer on AA6082 Al–Mg–Si aluminum alloy by electrical discharge alloying process”, Transactions of nonferrous metals society of china”, 26(12): 3205-3218 (2016)
16. P.Młynarczyk, D.Krajcarz, D.Bańkowski, “The Selected Properties of the Micro Electrical Discharge Alloying Process Using Tungsten Electrode on Aluminum”. Procedia. Engineer. 192:603-608 (2017).
17. H G.Lee, J. Simao, D K. Aspinwall, R C.Dewes and W.Voice , “Electrical discharge surface alloying”, Journal of Materials Processing Technology. 149(1-3):334-340 (2004)
18. R. Ramakrishnan and L. Karunamoorthy, “Multi response optimization of wire EDM operations using robust design of experiments”, International Journal of Advanced Manufacturing Technology. 29(1-2):105-112 (2006)
19. A. Haja Maideen, Muthukannan Duraiselvam, M. Varatharajulu, “Application of Desirability Function Approach for Optimized Process Parameters of Electrical Discharge Alloying of Al 7075 with Nickel Powder”, Transactions of the Indian Institute of Metals. 1-16 (2019)
20. I. Arun, P. Vaishnavi, M.Duraiselvam, S.Senthilkumar, V. Anandakrishnan , “Development of carbide intermetallic layer by electric discharge alloying on AISI-D2 tool steel and its wear resistance”, International journal of materials research. 105(6):544-551 (2014).
21. I.Arun, M.Duraiselvam, V.Senthilkumar, Narayanasamy and V.Anandakrishnan, “Synthesis of electric discharge alloyed nickel–tungsten coating on tool steel and its tribological studies”, Materials & Design. 63:257-262 (2014).
22. I. Arun, M. Durai Selvam and V.Senthilkumar, “Modelling and analysis of Electrical Discharge Alloying through Taguchi technique”, Applied. Mechanics and Materials. 64:592- 521 (2014).
23. Standard Test Method for Wear Testing with a Pin-on-Disk Apparatus: ASTM-G99-05 (2010).
24. S.Arooj, M.Shah, S.Sadiq, SHI. Jaffery, and S. Khushnood , “Effect of current in the EDM Machining of Aluminum 6061 T6 and its Effect on the Surface Morphology”, Arabian Journal for Science and Engineering.39(5):4187-4199 (2014).
25. I. Puertas, C J.Luis and L.Alvarez, “Analysis of the influence of EDM parameters on surface quality, MRR and EW of WC–Co”. Journal of Material Processing Technology. 153:1026-1032 (2004).
26. N L.Parthasarathi, M.Duraiselvam, and U. Borah, “Effect of plasma spraying parameter on wear resistance of NiCrBSiCFe plasma coatings on austenitic stainless steel at elevated temperatures at various loads”, Materials &. Design. 36:141-151 (2012).
27. M.Varatharajulu, G.Jayaprakash and N.Baskar, “Experimental investigation and multi objective optimisation of Duplex 2304 drilling operation using evolutionary algorithm”, International Journal of manufacturing technology and management 32: 336-357 (2018).
28. P. Prasanna, TVSSP.Sashank, B.Manikanta and P.Aluri, “Optimizing the Process Parameters of Electrical Discharge Machining On AA7075 - SiC Alloys”. Materials Today: Proceedings, 4(8): 8517–8527 (2014)

AUTHORS PROFILE

A. Haja Maideen, completed his Bachelor degree in Mechanical Engineering during 1994 – 1997. His Master degree in Production Engineering in Annamalai University, Chidambaram during 1997 - 1998. Currently, working as an Associate Professor in Department of Mechanical Engineering at A. V. C. College of Engineering, Mayiladuthurai. He is an author of 5 national and 2 international conferences and published a paper in the international journal. He is a life member in IIPE and ISTE. His areas of research interests is alloying of various new materials.

Dr.-Ing. M. Duraiselvam, received his B. E. degree in Mechanical Engineering from Coimbatore Institute of Technology, Coimbatore, India in 1996, M. E., Manufacturing Technology from National Institute of Technology, Tiruchirappalli, India in 1998, M. B. A. Operations Management, from Madurai Kamaraj University, Madurai, India in 2001. He got his Ph. D. from Technical University of Clausthal, Clausthal-Zellerfeld, Germany in 2006. Currently working as Professor in Dept of Production Engineering and Head in Siemens, Centre of Excellence. He is the Life Member - The Institution of Engineers (India). He had submitted more than fifty five research papers in international journals and twenty eight in international Conferences. So far, he produced 11 Ph.D Candidates and 09 ongoing Ph.Ds. Funds received from various funding agencies is of around 189 Lakhs and ongoing is 105 lakhs. His research areas of interest is Laser Surface Engineering, tribology and micromachining. Act as a reviewer in various peer review journal.

Dr, M. Varatharajulu, did his undergraduate Production Engineering at Adhiyamaan College of Engineering, Hosur, India postgraduate Computer Aided Design at the Bharathiyar College of Engineering and Technology, Karaikal. He carried out his research at Saranathan College of Engineering, Tiruchirappalli and completed his Ph.D. at the Anna University, Chennai. He has published 9 papers in national and international conferences and 16 papers in national and international journals. Currently he is an Assistant Professor at the A. V. C. College of Engineering, Mayiladuthurai, Tamilnadu, India. His research interests include optimization in various machining parameters, software development in mechanical design, finite element analysis and computational fluid dynamics.